Acta Cryst. (1980). B36, 2977–2985

The Structure of and Disorder in Dicalcium Barium Propionate

BY K. STADNICKA

Institute of Chemistry, Jagiellonian University, ul. Karasia 3, 30-060 *Kraków, Poland*

AND A. M. GLAZER

*Clarendon Laboratory, University of Oxford, Parks Road, Oxford OX*1 3*PU, England*

(*Received* 22 *January* 1980; *accepted* 11 *August* 1980)

Abstract

The room-temperature crystal structure of dicalcium barium propionate, $Ca_2Ba(C_2H_5COO)_6$, is described. It is cubic with $a = 18{\cdot}178\,(1)$ Å and space group $Fd3m$ (O_h^7); $R = 0{\cdot}0284$, $R_w = 0{\cdot}0238$, $R_G = 0{\cdot}0310$. The propionate molecules are found to be disordered between two sites. It is suggested that there are large-amplitude oscillations of the molecules about pseudo-twofold axes with occasional flipping of the methyl C atoms from one site to the other. Diffuse-scattering studies indicate correlations along ⟨110⟩ between the propionate groups with smaller correlations along ⟨001⟩. These are explained by an examination of the intermolecular contacts of the methyl C atoms, which shows that it is impossible to construct a fully three-dimensionally ordered structure.

Introduction

Over the last few years, interest in the dicalcium metal propionates [$Ca_2M(C_2H_5COO)_6$ with M = Ba, Pb or Sr] has grown because of the existence of ferroelectricity in some of their phases. In particular, it is known that dicalcium lead propionate (DLP) is ferroelectric at room temperature (Takashige, Iwamura, Hirotsu & Sawada, 1976), whereas the Sr compound (DSP) is ferroelectric below 281 K (Matthias & Remeika, 1957). However, no structural model for the ferroelectric behaviour has so far been developed, mainly because of the lack of a reliable structural analysis of this series of materials. The structures of both the paraelectric and ferroelectric phases of DSP have been published (Maruyama *et al.*, 1967; Mahalaxmi, 1968; Mizutani *et al.*, 1967), but the results are too imprecise to allow a good explanation of the physical properties to be proposed. The difficulty in structure determination here arises from the apparent disorder of certain methyl groups; moreover, the space groups are $P4_1$ (ferroelectric) and $P4_12_12$ (paraelectric) with four molecules per unit cell, resulting in a large number of general positions to be found. For example, refinement of the ferroelectric phase with anisotropic temperature factors requires up to 298 independent parameters, excluding H atoms.

It has been proposed that in both DLP and DSP there is a hypothetical cubic (prototype) phase of $Fd3m$ symmetry (Sawada, Ishibashi & Takagi, 1977) from which the actual structures are derived. The hypothetical transition to this phase is ferroelastic and the ferroic species is denoted $m3mF422$ in Aizu's (1969) notation. The Ba compound (DBP) is known to be cubic and early structural study indicated either $Fd3m$ (Nitta & Watanabe, 1935) or $F4_132$ (Biefeld & Harris, 1935) at room temperature. In both analyses, which were only partial, the metal positions were determined, with the Ba atoms forming an arrangement as in the diamond structure. The Ca atoms were found to lie tetrahedrally around the Ba atoms with the propionate molecules on pseudo-twofold axes directed along the molecular lengths [along the C(1)–C(2) bonds] and bisecting the O–C–O angles.

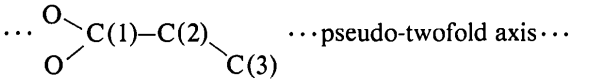

Because the methyl C atoms were not expected to lie along the same directions rotational disorder of the methyl groups about the long axis of the molecule was proposed.

Since these determinations were only carried out roughly and because of the likely connection with ferroelectric DLP and DSP, we felt that a detailed analysis of DBP would lead towards a better understanding of the physical properties of this system as a whole.

In DBP there are two low-temperature phase transitions. One is at 267 K and is of first order (Seki, Momotani & Nakatsu, 1951; Seki, Momotani, Nakatsu & Oshima, 1955) and the other is at 204 K and is of second order (Nakamura, Suga, Chihara & Seki, 1968; Kameyama, Ishibashi & Takagi, 1975). Although none of these phases seems to be ferroelectric, it is now known that a ferroelectric phase does appear in DBP at high pressure (Gesi & Ozawa, 1975; Sawada, Kikugawa & Ishibashi, 1979).

0567-7408/80/122977-09$01.00

In this paper, we present a new structural analysis of DBP and show that there is disorder in the propionate groups *as a whole* between *two* sites and that there are short-range correlations between these groups along the ⟨110⟩ and ⟨001⟩ directions. Other work on DBP (Nakamura, Suga, Chihara & Seki, 1968) and on the related DSP (Nakamura & Hosoya, 1967) and DLP (Yagi & Tatsuzaki, 1974) suggests dynamical disorder of the methyl groups, rather than static. We propose on this basis a reason for the observed correlations in DBP.

The structural study

Experimental

DBP crystals were grown by slow evaporation of an aqueous solution of the propionate salts in stoichiometric proportions. The resulting crystals were colourless, optically isotropic and octahedral in shape (often truncated on {100}). A preliminary examination with $0kl$ and $1kl$ Weissenberg photographs confirmed that they were all face-centred cubic.

A small crystal was ground to a sphere of about 0·35 mm diameter. Intensity data were collected at room temperature on an Enraf–Nonius CAD-4 diffractometer up to an angle of $\theta = 27°$ with graphite-monochromated Mo $K\alpha$ radiation. An $\omega/2\theta$ scanning mode was used, with the scan width varying as $0{\cdot}08° + 0{\cdot}30° \tan\theta$.

The cubic cell parameter was refined using the CAD-4 autoindexing procedure from the φ, χ, ω and 2θ setting angles of 15 reflections.

Deviations in the intensity of two standard reflections monitored after each group of 46 measurements were less than 2·5%. Lorentz–polarization and absorption corrections [$\mu_{\mathrm{Mo}K\alpha} = 1{\cdot}594$ mm^{-1}, *International Tables for X-ray Crystallography* (1959, p. 295)] were applied, but no extinction correction was attempted. Altogether 1707 reflections were measured above background.

Space group determination

In the earlier work there was much discussion about the possible space group of DBP. Nitta & Watanabe (1935) decided on $Fd3m$ (O_h^7) based on a combination of Laue and oscillation photographs. The assignment of space group $F4_132$ (O^4) by Biefeld & Harris (1935), on the other hand, is dubious as they gave no evidence for extra reflections of the type $0kl$ ($k + l \neq 4n$) which would distinguish $F4_132$ from $Fd3m$. Therefore, in the face of this confusion, we carefully re-examined all space-group possibilities.

Space groups $Fm3$ (T_h^3), $F432$ (O^3), $F\bar{4}3m$ (T_d^2) and $Fm3m$ (O_h^5) were eliminated since there were many systematic absences in addition to those caused by F-centring. Space groups $F\bar{4}3c$ (T_d^5), $Fm3c$ (O_h^6) and $Fd3c$ (O_h^8) could also be eliminated because of the presence of hhl reflections with $h(l)$ odd. The remaining space groups $F4_132$ (O^4), $Fd3m$ (O_h^7) and $Fd3$ (T_h^4) were examined in more detail. When a sort–merge procedure, using the program *SHELX* 76 (Sheldrick, 1976), was applied to the data with the assumption of $F4_132$, it was found that all 12 reflections of the type $h00$ ($h \neq 4n$), automatically rejected according to symmetry restrictions, had F_{obs} less than 4σ. The agreement for the resulting 567 unique merged reflections was $R = 0{\cdot}0124$. When the sort–merge procedure was used in $Fd3m$, 86 reflections were automatically rejected and 361 unique reflections resulted with $R = 0{\cdot}0120$. Of the rejected reflections 74 were of the type $0kl$ ($k + l \neq 4n$) and examination of these showed that their F_{obs} were less than 4σ. The other 12 reflections rejected were the same as in $F4_132$. We could therefore safely eliminate $F4_132$. Sort–merging with $Fd3$ gave the same 86 rejected reflections as in $Fd3m$, but because of the different Laue symmetry, $m3$, $R = 0{\cdot}0117$ and 565 unique reflections resulted. Examination of these reflections, however, showed that $m3m$ Laue symmetry was more appropriate, and this is supported by the close similarity in R factors for $Fd3m$ and $Fd3$ despite the large difference in numbers of unique reflections. We have therefore concluded that the correct space group is $Fd3m$ (O_h^7).

Crystal data

$Ca_2Ba(C_2H_5COO)_6$, $M_r = 655{\cdot}9$, cubic, space group $Fd3m$ (O_h^7), $a = 18{\cdot}178$ (1) Å, $V = 6007$ Å^3, $Z = 8$, $D_x = 1{\cdot}450$ Mg m^{-3}, $D_m = 1{\cdot}44$ (Biefeld & Harris, 1935), $D_m = 1{\cdot}45$ Mg m^{-3} (Nitta & Watanabe, 1935).

Refinement

Subsequent calculations were made with reflections with $F_{\mathrm{obs}} > 4\sigma(F_{\mathrm{obs}})$, resulting in the suppression of 12 more reflections to leave 349 unique reflections. Scattering factors for neutral atoms were taken from *International Tables for X-ray Crystallography* (1974, p. 99; f' and f'' from p. 149).

Patterson maps showed that the metal atoms were in the special positions given by the earlier workers, see Table 1. Fourier syntheses further revealed peaks corresponding to O and carboxyl C [C(1)] atoms in the following special positions, with respect to an origin $(-\frac{1}{8},-\frac{1}{8},-\frac{1}{8})$ from the inversion centre:

O in 96(g) (m) z,x,x *etc.*, with $x = 0{\cdot}037$ (0·042) and $z = 0{\cdot}148$ (0·160);

C(1) in 48(f) (mm) $x,0,0$ *etc.*, with $x = 0{\cdot}190$ (0·194).

The coordinates given in parentheses are those of Nitta & Watanabe.

Table 1. *Fractional coordinates, thermal parameters and bond lengths and angles*

Results of refinement *A*: O and C(1) in mean positions on the pseudo-twofold axis; C(2) and C(3) with half weight on either side of the pseudo-twofold axis

Results of refinement *B*: O, C(1), C(2) and C(3) with half weight on either side of the pseudo-twofold axis.

Refinement *A*: $R = 0.0284$; $R_w = 0.0238$; $R_G = 0.0310$
Refinement *B*: $R = 0.0246$; $R_w = 0.0193$; $R_G = 0.0261$

(*a*) Fractional coordinates (asterisks indicate atoms with half site-occupancy factor)

	Site	Point symmetry	x	$y = z$
Refinement *A*				
Ba	8(*a*)	$\bar{4}3m$	0	0
Ca	16(*c*)	$\bar{3}m$	$\frac{1}{8}$	$\frac{1}{8}$
O	96(*g*)	*m*	0·1532 (3)	0·0397 (1)
C(1)	48(*f*)	*mm*	0·1886 (4)	0
C(2)*	96(*g*)	*m*	0·2714 (7)	0·0175 (7)
C(3)*	96(*g*)	*m*	0·3191 (9)	−0·0233 (7)
Refinement *B*				
O(1)*	96(*g*)	*m*	0·1447 (4)	0·0409 (7)
O(2)*	96(*g*)	*m*	0·1663 (7)	−0·0386 (7)
C(1)*	96(*g*)	*m*	0·1869 (5)	0·0038 (10)
C(2)*	96(*g*)	*m*	0·2710 (6)	0·0173 (6)
C(3)*	96(*g*)	*m*	0·3193 (8)	−0·0228 (6)

(*b*) Temperature factors (Å²)

$$T = \exp[-2\pi^2(U_{11}h^2a^{*2} + \ldots 2U_{12}hka^*b^* + \ldots)]$$

	U_{11}	$U_{22} = U_{33}$	U_{23}	$U_{13} = U_{12}$
Refinement *A*				
Ba	0·0456 (2)	0·0456 (2)	0	0
Ca	0·0924 (7)	0·0924 (7)	−0·0281 (6)	−0·0281 (6)
O	0·124 (3)	0·188 (3)	−0·113 (3)	−0·006 (2)
C(1)	0·068 (4)	0·155 (5)	−0·042 (6)	0
C(2)	0·068 (5)	0·308 (9)	−0·136 (9)	0·009 (6)
C(3)	0·108 (7)	0·328 (9)	−0·083 (9)	0·058 (7)
Refinement *B*				
Ba	0·0457 (2)	0·0457 (2)	0	0
Ca	0·0924 (6)	0·0924 (6)	−0·0279 (5)	−0·0279 (5)
O(1)	0·054 (3)	0·209 (4)	−0·143 (4)	−0·005 (2)
O(2)	0·142 (6)	0·162 (4)	−0·083 (4)	−0·003 (5)
C(1)	0·079 (4)	0·150 (4)	−0·050 (5)	−0·032 (5)
C(2)	0·063 (4)	0·313 (6)	−0·145 (6)	0·013 (4)
C(3)	0·110 (5)	0·326 (6)	−0·085 (6)	0·053 (4)

Parameter correlation over 50%

Refinement *A*:	Scale	U_{11}(Ba)	83%
	U_{11}(Ca)	U_{23}(Ca)	−61
	U_{22}(O)	U_{23}(O)	−72
Refinement *B*:	Scale	U_{11}(Ba)	81
	U_{11}(Ca)	U_{23}(Ca)	−61
	y[O(1)]	y[O(2)]	92
	y[O(1)]	U_{13}[O(2)]	−77
	U_{13}[O(1)]	y[O(2)]	58
	y[C(1)]	U_{22}[C(1)]	−53
	y[C(1)]	x[C(1)]	−63
	y[O(2)]	U_{13}[O(2)]	−70
	x[O(1)]	U_{11}[O(2)]	58
	U_{11}[O(1)]	x[O(2)]	−51

Table 1 (*cont.*)

(*c*) Bond lengths (Å) and angles (°)

Refinement *A*			
Ba–O	2·965 (5)	Ca–O	2·253 (4)
O–O′	2·039 (8)	O–C(1)	1·205 (5)
C(2)–C(1)–O	105·6 (7)	C(2)–C(3)	1·36 (2)
O–C(1)–O′	115·5 (8)	C(2)–C(1)–O′	139·0 (8)
	Ca–O–Ba	97·0 (2)	
	C(1)–C(2)	1·57 (2)	
	C(3)–C(2)–C(1)	113 (1)	
Refinement *B*			
Ba–O(1)	2·834 (9)	Ba–O(2)	3·182 (9)
O(1)–O(2)	2·08 (1)	C(1)–C(2)	1·57 (1)
O(2)–C(1)	1·15 (3)	C(3)–C(2)–C(1)	118 (1)
Ca–O(1)–Ba	102·4 (4)	O(1)–C(1)–C(2)	116 (2)
O(1)–C(1)–O(2)	122 (1)		
Ca–O(1)	2·19 (2)	Ca–O(2)	2·35 (2)
O(1)–C(1)	1·22 (3)	Ca–O(2)–Ba	89·5 (4)
C(2)–C(3)	1·36 (2)	O(2)–C(1)–C(2)	122 (2)

These fractional coordinates were then refined by full-matrix least squares, using the *SHELX* 76 program, including anisotropic temperature factors for Ba and Ca and isotropic temperature factors for O and C(1). After five cycles the agreement factors were $R = \sum|\Delta F|/\sum|F_{obs}| = 0.1056$, $R_w = \sum w^{1/2}|\Delta F|/\sum w^{1/2}|F_{obs}| = 0.0925$, $R_G = [\sum w(\Delta F)^2/\sum wF_{obs}^2]^{1/2} = 0.1624$, with a weighting scheme based on counting statistics according to $w = k[\sigma^2(F_{obs})]^{-1}$.

A difference Fourier synthesis showed a large amount of electron density centred on the twofold axis corresponding to the region where C(2) and C(3) should lie. Fig. 1(*a*) shows this region in detail viewed down on to $(01\bar{1})$, *i.e.* the molecular plane defined by C(1) and the O atoms. It can be seen that the density is very spread out with a minimum in the middle. A cross section (Fig. 1*b*) shows maxima separated in the molecular plane and the general overall shape of the contours is flattened in this plane. In order to understand this we must consider molecular disorder.* Hitherto, only disorder in the methyl group has been proposed, but it is evident from these maps that the situation is more complicated.

First of all, in order to see why the C(2)–C(3) density is appreciably flattened in the molecular plane defined by C(1) and the two O atoms, a model was constructed. From this it was found that if the methyl group is allowed to rotate about the C(1)–C(2) bond there would be a strong steric interaction with methyl groups on other propionates. This suggested that the methyl group most likely lies roughly in the molecular plane so as to maximize its distance from other methyl

* We use the term 'disorder' here in a general sense to denote either static or dynamic fluctuations. Similarly, thermal ellipsoids may be considered as arising from either disorder.

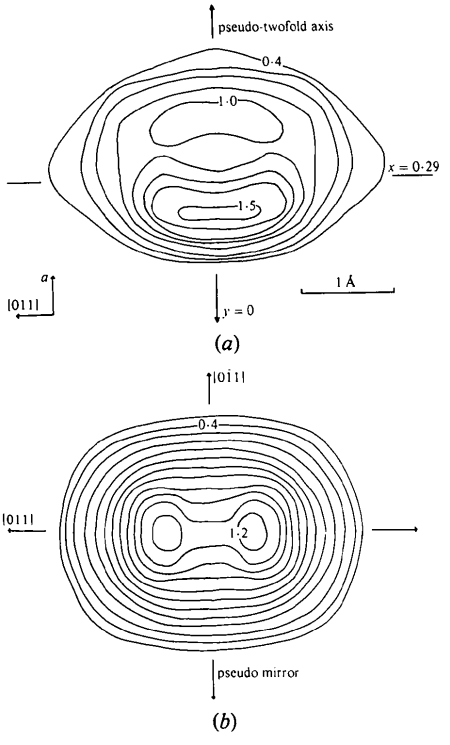

Fig. 1. (*a*) Difference electron density map in the propionate molecular plane. Here, the region between $x = 0{\cdot}25$–$0{\cdot}37$ is shown for a molecule lying along [100]. The molecular plane is $(01\bar{1})$. The electron densities in e Å^{-3} are marked on the contours. (*b*) Section of the difference electron density of (*a*) taken along $x = 0{\cdot}29$ and viewed along [100].

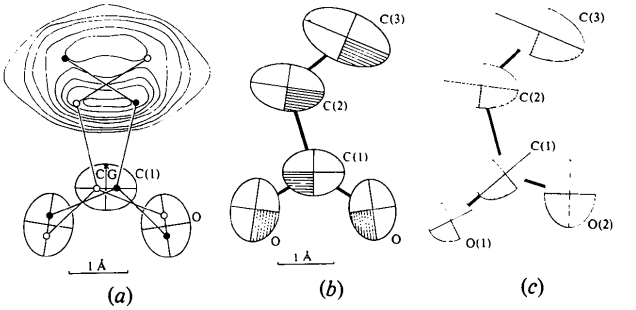

Fig. 2. (*a*) Two propionate groups superimposed on the difference electron density of Fig. 1(*a*) and on the refined thermal ellipsoids of O and C(1). The orientations of both groups have been adjusted by rotating them about their common centre of gravity so as to give the best fit. (*b*) The refined thermal ellipsoids of O, C(1), C(2) and C(3), with disordering of C(2) and C(3) assumed, and with O and C(1) in their mean positions (refinement *A*). (*c*) The same as in (*b*) but with O, C(1), C(2) and C(3) all assumed disordered (refinement *B*).

groups. It is worth noting that also in the structure of propionic acid (Strieter, Templeton, Scheuerman & Sass, 1962) the methyl group lies in the molecular plane. Since the space group introduces a twofold axis along the molecular length the methyl group must on average occur on both sides of this axis but with half weight. This should be compared with the earlier structural studies, as well as with the results of magnetic-resonance experiments (Nakamura, Suga, Chihara & Seki, 1968) where a dynamic rotation of the methyl group about the pseudo-twofold axis was proposed. The main difference here is that we do not have free rotation but a two-site disorder (either static or dynamic flipping). Similarly we see that since the density due to C(2) is also spread out we must consider a similar disorder for this atom too.

In order to understand the disorder further, we considered that, by analogy with normal modes of vibration, the pseudo-twofold axis, about which the disordering or flipping takes place, should pass through the centre of gravity of the molecule. In Fig. 2(*a*) we show the two possible positions of the molecule adjusted to fit C(2) and C(3) on to the density contours with the centre of gravity of the molecule constrained to lie on the pseudo-twofold axis. Also shown are the thermal ellipsoids of O and C(1) obtained. We see that the O and C(1) atoms of the two disordered molecules fit extremely well on to the ellipsoids computed for average O and C(1), and, moreover, we can even understand why the O ellipsoids are elongated in the molecular plane and pointing in a direction about 10° away from the pseudo-twofold axis. In Fig. 2(*b*) and Table 1 we show the resulting positions and thermal ellipsoids after refining all atoms (no attempt was made to include H atoms because of the large amount of disorder), assuming average O and C(1) atoms and including disordered C(2) and C(3) with half weight either side of the pseudo-twofold axis (refinement *A*). The refined positions agree well with those proposed in Fig. 2(*a*) and this, together with the very low *R* factors obtained, supports our disorder model. The refined thermal ellipsoids for C(2) and C(3) in Table 1 also describe very well the overall shape of the difference density observed. Thus our observations strongly indicate that it is the *whole* molecule that should be considered to be disordered, rather than simply the C(2) and C(3) atoms alone, although the disordering effect is smaller for C(1) and O.

Several cycles of refinement with all propionate atoms distributed on both sides of the pseudo-twofold axis (refinement *B*) were also carried out and the results are included in Table 1 for comparision. It is not easy to decide which of these two refinements represents the most reliable description of the structure. Both give extremely low *R* factors but when we apply Hamilton's (1965) significance test, we find that R_w(model *A*)/R_w(model *B*) = 1·233: testing for the hypothesis that model *A* describes the true structure we find that $\mathscr{R}_{27,314,0.005} = 1{\cdot}091$, *i.e.* a rejection of the hypothesis at the 0·005 level. However, in refinement *B* there are more high correlations between the parameters. In particular, there is a 92% correlation between y[O(1)]

and y[O(2)] and significant correlations between the O y coordinates and the temperature factors. Even x[C(1)] is affected, and so the C(1) and O parameters derived from refinement B may not be realistic. Fig. 2(*c*) shows the refined propionate molecule in this case and we see that the O ellipsoids are rather oddly oriented. Given the high correlations it is not possible to decide whether these are real or artifactual. In the following sections, therefore, unless specifically stated otherwise, we shall confine ourselves to the results of refinement A.*

Description of the structure

The structure, because of its high pseudo-symmetry and large unit cell, is very complicated to describe succinctly. Fig. 3 shows a stereopair of a section of the structure: here, for simplicity, the C(3) atoms have been omitted and C(2) and C(1) are placed directly on the pseudo-twofold axes. Fig. 4 shows a projection of the refined structure (refinement A) of a narrower section for comparison, and Fig 5 shows the coordination around Ba and Ca in more detail. From Figs. 3 and 4 it can be seen that six propionate groups octahedrally surround the Ba atoms with their O atoms closest, *i.e.* there are 12 O atoms closest to and equidistant from Ba. The O coordination polyhedron around Ba has eight faces, which can be described as a combination of two tetrahedra, one bigger than the other (Fig. 5*b*). The Ca atom is surrounded by six O atoms from six different propionate groups to form a trigonal antiprism (Fig. 5*b*). If it is assumed that the propionate molecule is dipolar with a negative charge on the O end it is understandable that the Ca–O bond should be so short (2·253 Å), suggesting that it is this interaction that is primarily responsible for holding the structure together. Indeed, it appears that the bond is so strong that a considerable amount of disorder is permitted at the other end of the propionate molecule.

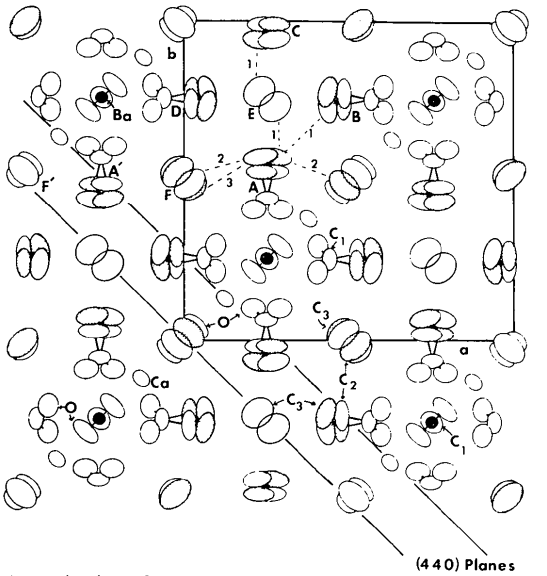

Fig. 4. Projection of a section of the structure from refinement A on to (001) with $z = 0{\cdot}175 \pm 0{\cdot}125$. Thermal ellipsoids are drawn for each atom with C(2) and C(3) shown in both disordered sites either side of the pseudo-twofold axis. The shading indicates one ordered arrangement of C(3) and C(2) if it is assumed that intermolecular C(3)–C(3) contacts are maximized. The distances marked are (1) 4·052, (2) 4·195, (3) 4·395 Å.

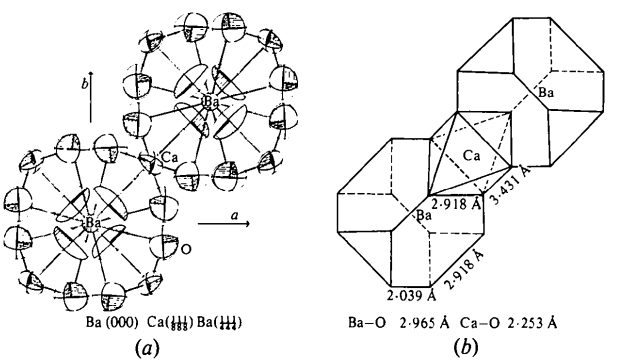

Fig. 5. The coordination of Ba and Ca by O. (*a*) Thermal ellipsoids are shown for each atom. (*b*) Coordination polyhedra of O atoms around Ba and Ca.

* Lists of structure factors for refinements A and B have been deposited with the British Library Lending Division as Supplementary Publication No. SUP 35545 (7 pp.). Copies may be obtained through The Executive Secretary, International Union of Crystallography, 5 Abbey Square, Chester CH1 2HU, England.

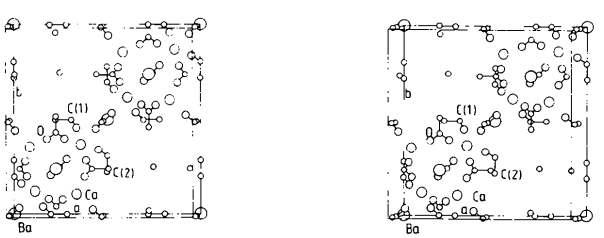

Fig. 3. Stereoplot of the idealized DBP structure between $z = 0$ and $z = 0{\cdot}49$. C(3) atoms are not shown.

It can also be seen from these diagrams that the propionate groups lie on {110} planes, so that around any particular Ba opposite propionate molecular planes are skewed 90° to each other. In addition, the long axes of the propionate molecules pass across 4_1 and 4_3 axes through $(\frac{1}{4},0,0)$, $(0,\frac{1}{4},0)$, *etc.*, and so they are found on regular layers along ⟨001⟩ but successively rotated through 90° about ⟨001⟩.

The bond lengths (Å) given in Table 1 can be compared with those found in propionic acid:

	propionic acid	refinement A	refinement B
C(1)–O	1·23 (1)	1·205 (5)	1·15 (3)
	1·32 (1)		1·22 (3)
C(2)–C(1)	1·50 (1)	1·57 (2)	1·57 (1)
C(3)–C(2)	1·54 (1)	1·36 (2)	1·36 (2).

The C–O distances found in DBP are reasonably similar to those in propionic acid, but C(3)–C(2) is shorter. However, this is hardly surprising given the unusually large 'apparent' thermal ellipsoids that have been obtained.

The C(3)–C(2)–C(1) angle in refinement *A* is precisely the same as that in propionic acid, whereas in refinement *B* it is 5° larger, again suggesting refinement *A* may have given the more realistic results.

Discussion of thermal ellipsoids

From the eigenvalues and eigenvectors of the thermal ellipsoids it is found that the ellipsoid axes are extremely large, especially for O, C(2) and C(3). This is shown in the stereoplot for refinement *A* in Fig. 6 as well as in the preceding figures. The largest apparent motion of atoms in the propionate molecule is in all cases in a plane perpendicular to the molecular axis. For the O atom the largest displacement is perpendicular to the molecular plane. The second-largest displacement points about 10° away from the molecular axis, as seen in Fig. 2(*b*), and was explained earlier by the disorder of the O atoms. The displacements of C(1) are more disc-like and smaller in magnitude, whereas those for C(2) and C(3) are much larger with the largest values perpendicular to the molecular plane. Some of the observed amplitude may be caused by the neglect of the H atoms, but since they too are certainly disordered their contribution will be small.

This is consistent with a model in which the whole molecule occupies, on average, not two exact sites about the pseudo-twofold axis, but two *ranges* of sites. Since, as mentioned earlier, the C(3) atom cannot spend much of its time above or below the observed average molecular plane, where it would be too close to C(3) atoms on neighbouring propionate groups, we can suppose that it spends most time in a range of positions distributed about the average refined position. If we take the disorder to be dynamic, rather than static, the picture is one in which the molecule executes a large-amplitude vibration as a whole about the pseudo-twofold axis, thus giving rise to the large out-of-plane ellipsoid axis for C(3), C(2) and O and the correspondingly smaller value for C(1), which is closer to this axis. This motion corresponds to one of the normal modes expected for the propionate group and this would explain why the disorder takes place with respect to the centre of gravity, described earlier. It is tempting to suggest that in DBP the whole molecule oscillates about the pseudo-twofold axis with such a large amplitude that occasionally the molecule rotates to its second position. However, it seems unlikely that the *whole* molecule turns over in this process, especially since there must be strong Ca–O bonding holding the O atoms in position; instead it is more energetically probable that it is C(3) and possibly C(2) (which are more free to move) that actually flip over to their alternative sites and that the rest of the molecule simply rotates slightly, about a line normal to the average molecular plane, to its alternative site. We would therefore predict the existence of a high-frequency mode, caused by the oscillation of the propionate molecule, and a low-frequency flipping of the molecule [principally C(3) and C(2)] between its alternative sites.

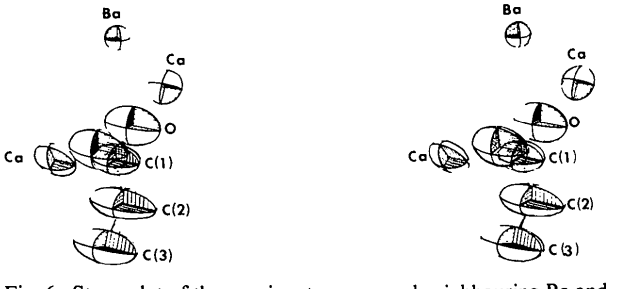

Fig. 6. Stereoplot of the propionate group and neighbouring Ba and Ca (refinement *A*).

Diffuse scattering

The observation of such a large degree of disorder in DBP prompted us to look for X-ray diffuse scattering. A series of stationary-crystal photographs were taken at 5° intervals about [001], using Cu radiation. Fig. 7 shows examples of these photographs, where it is apparent that there are many diffuse streaks. The positions of diffuse maxima were measured by the method described by Glazer (1970) and plotted in reciprocal space. Fig. 8 shows the resulting *hk*0, *hk*2 and *hk*4 sections. *hkl* sections with $l = 1, 3$ do not show much diffuse scattering except where streaks from other layers pass through. It can be seen that the streaks are all directed along $\langle 110 \rangle$ directions. In *hk*0 they mainly pass through 440, 880, *etc.*, *i.e.* with the relationship $h + k + l = 8n$. Similarly, in *hk*4 they pass through $h + k + l = 8n$. However, in *hk*2 they are given by $h + k + l = 4n$ and so are closely spaced. Similar streaking has been observed in diamond, silicon and germanium (Honjo, Kodera & Kitamura, 1964; Komatsu & Teramoto, 1966), only there all the streaks obey $h + k + l = 4n$. Cross sections of, say, the $[1\bar{1}0]$ streaks in DBP (Fig. 7) show them to be elongated along [001], so that they are actually planes of diffuse scattering, infinite in $[1\bar{1}0]$, sharp in [110] and extended but finite in [001].

In order to understand the origin of these streaks we considered our refined structure. Since most of the disorder found in DBP is shown by C(3) [and C(2)] it is very likely that the propionate groups are the main contributors to the diffuse scattering. We can, by considering the propionate groups alone, explain the presence or absence of the different streaks. From Fig. 4 it is seen that the propionate groups all lie along

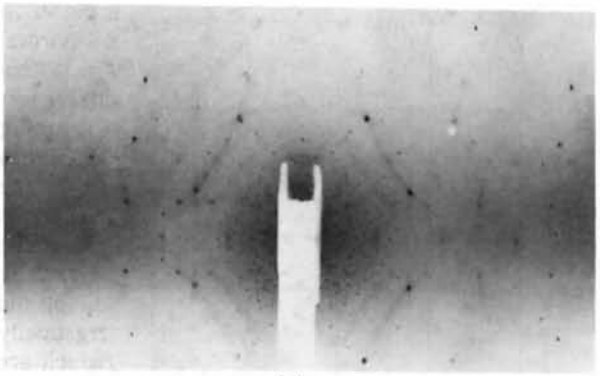

(*a*)

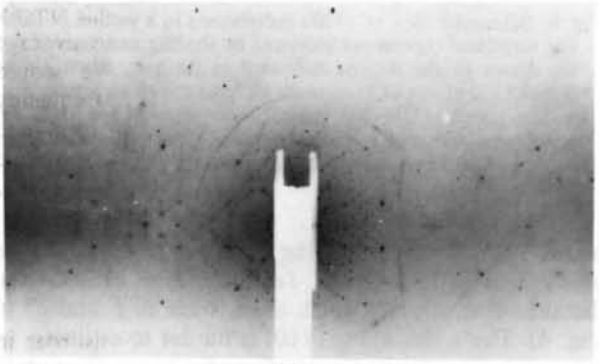

(*b*)

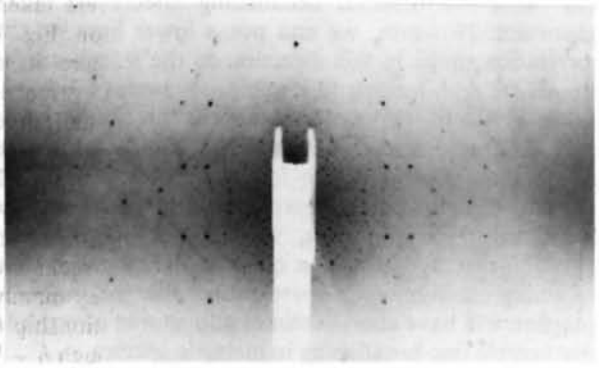

(*c*)

Fig. 7. Stationary-crystal photographs about [001]. (Cu radiation, unfiltered, 1 h exposures.) (*a*) Beam along [100]. (*b*) Beam 15° from [100]. (*c*) Beam along [110].

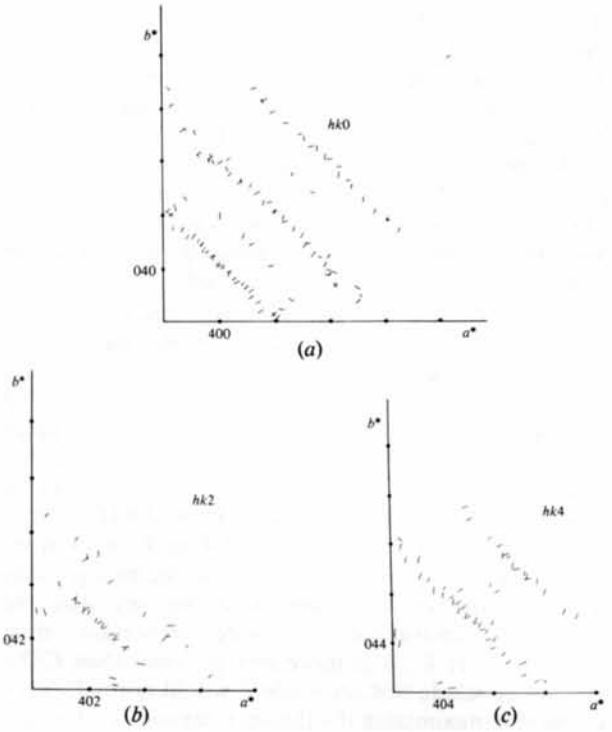

Fig. 8. Distribution of diffuse scattering in (*a*) *hk*0, (*b*) *hk*2 and (*c*) *hk*4 reciprocal-lattice sections.

$\langle 110 \rangle$, *i.e.* along directions parallel to the streaks. Now, if we have streaks along $[1\bar{1}0]$ passing through the reciprocal-lattice point *hhl* we find the direction [*uvw*] perpendicular to reciprocal-lattice vectors $d^*_{1\bar{1}0}$ and d^*_{hhl}. As a reciprocal-lattice section containing these two vectors is the zero layer for the [*uvw*] direction the scattering on this plane results from a projection of the structure down [*uvw*]. Thus for the streak passing through 440 in *hk*0 we project the structure down [001]. As each propionate group is related to each point $(\frac{1}{4},0,0)$, $(0,\frac{1}{4},0)$ *etc.* in the crystal, a projection of all such points down [001] shows them all to lie on (440) planes. These planes have been marked on Fig. 4, thus showing that it is the propionate groups that cause the diffuse streaks through 440, 880, *etc.*, as suspected earlier. To explain the streak through 552 we project these same points down $[11\bar{5}]$ and once again find that they lie on (552) planes [as well as (10,10,4)]. For the 664 streak we project down $[11\bar{3}]$ to find the same points on (664) planes. In this way we can demonstrate the origins of all the streaks observed.

Let us take the section of the structure in Fig. 4 and assume at some point in time that one of the molecules (*A*) is in one of its two possible sites. This brings its methyl carbon [C(3)*A*] to within 4·052 Å of one of the two possible C(3)*B* sites. This is a considerably smaller distance than is possible $\{2 \times [(\text{C}-\text{H}) + r_{\text{H}}(\text{van der Waals})] \simeq 4{\cdot}5$ Å$\}$ and so C(3)*B* cannot occupy this site. It is therefore forced to lie in its other position at a distance of 4·765 Å. This C(3) then causes a similar effect to molecule *C* and this in turn to molecule *D*. Therefore, having fixed the site of molecule *A*, molecules *B*, *C* and *D* are forced to take on an ordered arrangement. However, C(3)*E*, which lies below the average plane containing *A*, *B*, *C* and *D*, cannot be determined unambiguously, as in one position it is 4·052 Å from C(3)*A* and in its other position the *same* distance to C(3)*C*. Similarly, the molecule *E'* directly above (not shown) also cannot be ordered uniquely. We see, therefore, that it is physically *impossible* to form a

completely ordered structure based on propionate molecules in this arrangement, and this is presumably why the degree of disorder is so large. At some other point in time (or in some other part of the structure) there can be ordering between molecules *A*, *E*, *C* and *E'*, but not then at the same time with molecules *B* and *D*. Therefore, our picture of the structure is one in which there are small planar regions of ordered propionates which are either changing dynamically or occur in different regions of the crystal.

Returning now to the ordered arrangement of molecules *A*, *B*, *C* and *D* we can consider its effect on the neighbouring propionate *F*. Here the distance from C(3)*A* to C(3)*F* is either 4·395 or 4·916 Å, depending on which site is chosen for *F*. However, if we place C(3)*F* at the site 4·916 Å from C(3)*A* we find that C(2)*F* is now at a distance of 4·195 Å from C(3)*A*. If C(2)*F* is placed in its alternative site at 4·610 Å from C(3)*A*, then we have to place C(3)*F* at 4·395 Å from C(3)*A*. There is thus an ambiguity in the two possible sites of molecule *F*. However, if we say that the C(3)–C(3) interaction is more important than C(3)–C(2) [as C(3) is more free to move than C(2)] then we conclude that molecule *F* would normally take up the site maximizing the distance between C(3)*F* and C(3)*A*. This would then similarly affect the next group of four propionates ($-a/2$, $-b/2$, 0) from the first group, thus forming a correlated chain along [110]. Fig. 4 shows an ordered arrangement of propionates in which the correlated chains extend simultaneously along [110] and [1$\bar{1}$0] [shaded C(2) and C(3)]. Bearing in mind that molecule *F* is the weak link in the chain with its ambiguity of positions, it is likely that the correlation ends at such a molecule, and so it would be unusual to have complete correlation over a long distance along [110] and [1$\bar{1}$0] at the same time. Thus we expect the correlations to tend to be linear, mainly independently along [110] or [1$\bar{1}$0]. This is schematically shown in Fig. 9. Of course in three dimensions these correlations will be along all ⟨110⟩ directions, more or less independently from one another. If the disorder is dynamic, the correlations represent propagation distances of phonons with wavevectors along ⟨110⟩. If we consider the possibility of correlation along ⟨100⟩ we find that there are more of the weak links, such as *F* (see Fig. 4, molecules *A*, *F*, *A'*, *F'*), in these directions. and so while there is some correlation along these directions it will be of shorter range than along [110]. Therefore, a long correlation along [110], say, and a shorter correlation along [001] with little or no correlation along [1$\bar{1}$0] would give rise to diffuse scattering in the form of narrow sheets perpendicular to [110] of limited extent along [001] and infinite along [1$\bar{1}$0], as indeed is found.

A very rough idea of the correlation lengths or propagation distances can be obtained from the streak widths. For a streak along [1$\bar{1}$0] the width along [00$\bar{1}$]

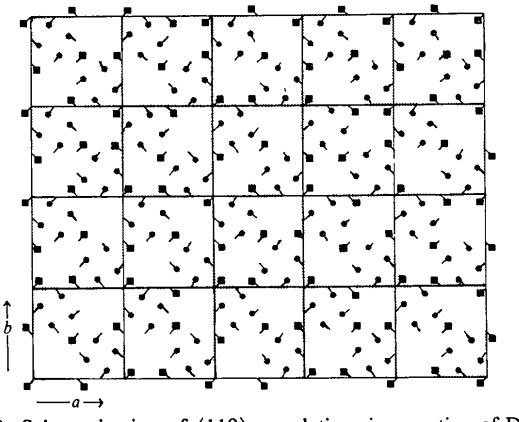

Fig. 9. Schematic view of ⟨110⟩ correlations in a section of DBP. The correlated regions are indicated by shading and, on average, are drawn to the lengths estimated in the text. Black circles denote C(3) atoms of propionate molecules with molecular axes in the plane of the diagram. Black squares are C(3) for propionates with molecular axes perpendicular to the plane of the paper, and are weak links in the correlation.

is $\simeq$0·11 Å^{-1}, corresponding to a correlation distance along [001] of about 9 Å, *i.e.* half a unit cell (*i.e.* the distance between two weak links, such as *F* and *F'* in Fig. 4). The width along [110] is harder to estimate, as it is rather narrow and corrections for beam divergence and other instrumental broadening effects are more important. However, we can put a lower limit on the correlation range in this direction as the streak widths are $\simeq$0·02 Å^{-1}, leading to a minimum average distance along [110] of about 50 Å, approximately two unit cells. Diffractometer measurements will be needed to give a more precise figure for this correlation length. These estimates have been used in drawing the correlated regions in Fig. 9. We see that the propagation distances may be quite short and, therefore, assuming a dynamic correlation, the phonons in question will have short lifetimes and should give rise to appreciable line-broadening in inelastic spectra.

Conclusions

We have shown that the structure of DBP is considerably more complex than hitherto thought. In particular, the earlier picture of a rotational disorder of the methyl groups must be replaced by a flipping of the *whole* molecule roughly between two sites. This picture suggests the possibility of two frequency regimes in the molecular motion, a slow flipping of the molecule and a higher-frequency oscillation of the molecule about the pseudo-twofold axis, which should be observable in Brillouin or photon-correlation spectroscopy.

The motion of the molecules appears to be strongly correlated in independent chains along all ⟨110⟩ directions and this has been explained by considering

intermolecular contacts between methyl C atoms. It is particularly remarkable that this consideration demonstrates clearly that *in this crystal there is no possibility of creating a fully three-dimensionally ordered crystal!* It is tempting to conclude from this that to produce an ordered structure the unit cell must distort to remove steric interactions and this may be the driving force for the phase transitions in this type of compound. It should be realized that the observed disorder, which gives an average space group $Fd3m$, can be explained in terms of twinning (dynamic or static) at the microdomain level, *i.e.* below the coherence length of X-rays, with each domain adopting either $P4_12_12$ or $P4_32_12$ symmetry. Thus the room-temperature structure consists of an intimate mixture of opposite chiralities. The low-temperature phase is expected, by analogy with DLP and DSP, to adopt a particular handedness, except with respect to large-scale domains. Therefore, the 267 K transition in DBP should be drastic, as is indeed found, since microdomains of a particular chirality must suddenly grow into macrodomains of the same chirality at the expense of microdomains of opposite chirality. Obviously, large movements of the propionate groups are necessary to accomplish this. It would be extremely interesting in this context to study the diffuse scattering as a function of temperature and pressure to see how the correlations change on approaching the phase transitions in DBP. This would very likely throw light on the transitions and properties of DLP and DSP.

We wish to thank Mr S. Singh for supplying the DBP crystals and Mr F. Wondre for taking the diffuse-scattering photographs. Useful comments from Dr I. G. Wood are appreciated. One of us (AMG) is grateful to the Jagiellonian University for an invitation to carry out much of this work in Poland and to Jesus College, Oxford, for a travel grant. We also thank the X-ray Laboratory of ŚLAFiBS, Kraków, for making the diffractometer available.

References

AIZU, K. (1969). *J. Phys. Soc. Jpn*, **27**, 387–396

BIEFELD, L. P. & HARRIS, P. M. (1935). *J. Am. Chem. Soc.* **57**, 396–399.

GESI, K. & OZAWA, K. (1975). *J. Phys. Soc. Jpn*, **38**, 467–470.

GLAZER, A. M. (1970). *Philos. Trans. R. Soc. London*, **266**, 635–639.

HAMILTON, W. (1965). *Acta Cryst.* **18**, 502–510.

HONJO, G., KODERA, S. & KITAMURA, N. (1964). *J. Phys. Soc. Jpn*, **19**, 351–366.

International Tables for X-ray Crystallography (1959). Vol. II. Birmingham: Kynoch Press.

International Tables for X-ray Crystallography (1974). Vol. IV. Birmingham: Kynoch Press.

KAMEYAMA, H., ISHIBASHI, Y. & TAKAGI, Y. (1975) *J. Phys. Soc. Jpn*, **38**, 1703–1707.

KOMATSU, K. & TERAMOTO, K. (1966). *J. Phys. Soc. Jpn*, **21**, 1152–1159.

MAHALAXMI, V. (1968). Thesis, Rensselaer Polytechnic Institute, USA.

MARUYAMA, H., TOMIIE, Y., MIZUTANI, I., YAMAZAKI, Y., UESU, Y., YAMADA, N. & KOBAYASHI, J. (1967). *J. Phys. Soc. Jpn*, **23**, 899.

MATTHIAS, D. T. & REMEIKA, J. P. (1957). *Phys. Rev.* **107**, 1727.

MIZUTANI, I., YAMAZAKI, Y., UESU, Y., YAMADA, N., KOBAYASHI, J., MARUYAMA, H. & TOMIIE, Y. (1967). *J. Phys. Soc. Jpn*, **23**, 900.

NAKAMURA, E. & HOSOYA, M. (1967). *J. Phys. Soc. Jpn*, **23**, 844–847.

NAKAMURA, N., SUGA, H., CHIHARA, H. & SEKI, S. (1968). *Bull. Chem. Soc. Jpn*, **41**, 291–296.

NITTA, I. & WATANABE, T. (1935). *Sci. Pap. Inst. Phys. Chem. Res. Jpn*, **26**, 164–177.

SAWADA, A., ISHIBASHI, Y. & TAKAGI, Y. (1977). *J. Phys. Soc. Jpn*, **43**, 195–203.

SAWADA, A., KIKUGAWA, T. & ISHIBASHI, Y. (1979). *J. Phys. Soc. Jpn*, **46**, 871–875.

SEKI, S., MOMOTANI, M. & NAKATSU, K. (1951). *J. Chem. Phys.* **19**, 1061–1062.

SEKI, S., MOMOTANI, M., NAKATSU, K. & OSHIMA, T. (1955). *Bull. Chem. Soc. Jpn*, **28**, 411–416.

SHELDRICK, G. M. (1976). *SHELX* 76. A program for crystal structure determination. Univ. of Cambridge, England.

STRIETER, F. J., TEMPLETON, D. H., SCHEUERMAN, R. F. & SASS, R. L. (1962). *Acta Cryst.* **15**, 1233–1239.

TAKASHIGE, M., IWAMURA, H., HIROTSU, S. & SAWADA, S. (1976). *Ferroelectrics*, **11**, 431.

YAGI, T. & TATSUZAKI, I. (1974). *J. Phys. Soc. Jpn*, **37**, 1038–1043.